Institute for Fusion Studies

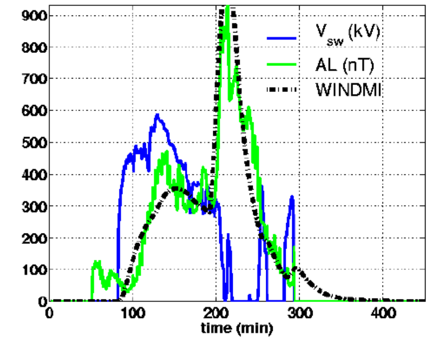

Nonlinear Ionospheric Turbulence and Magnetic Substorms Driven by the Solar Wind

W. Horton and L. Mays

University of Texas at Austin

E. A. Spencer

Utah State University, Logan, Utah

Modern Challenges in Nonlinear Plasma Physics

June 15-19, 2009

Halkidiki, Greece

www.astro.auth.gr/~vlahos/kp/

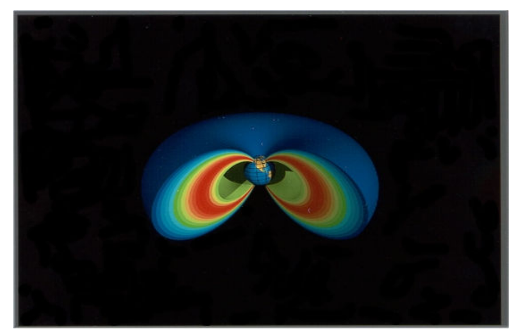

Outline

Dynamics Driven by Solar Wind in Magnetosphere-Ionosphere System

- Drift-ballooning Interchange Modes
- Reconnection dynamics from Tearing Modes
- BBFs, Firehose Instability and Pi2 signals
- Polar Cap Convection and the Gradient Drift Instability = GDI

Issues:

Q1. How to connect the complex, distributed dynamics of the magnetosphere-ionospheric (MI) system? (integrated system dynamics)

Q2. How to describe the substorms and dipolarization fronts with the associated kinetic instabilities, ring current energization, and acceleration of MeV electrons?

Southward IMFdrives MRC, the Two-Cell polar cap convection and inward geotail convection

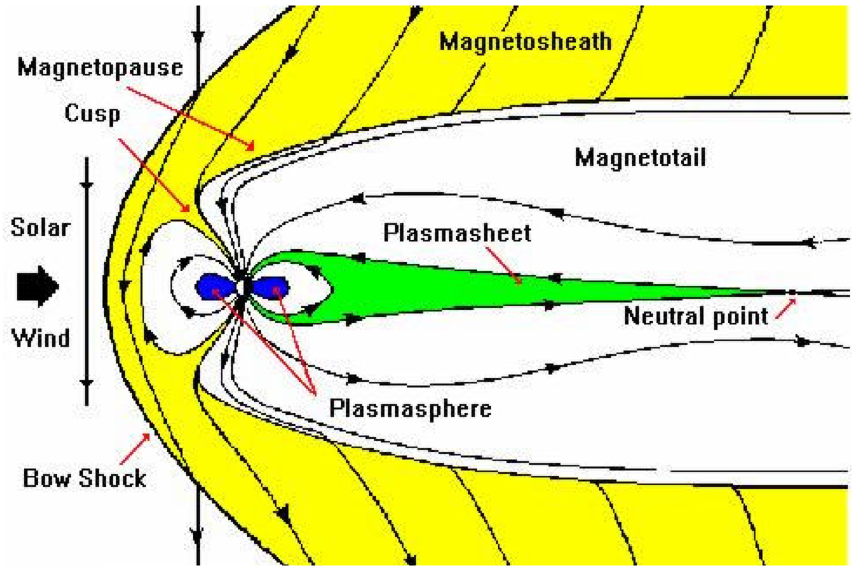

PLASMA FLOW DUE TO THE ELECTRIC FIELDS

Polar Cap Convection

Driven by Solar Wind

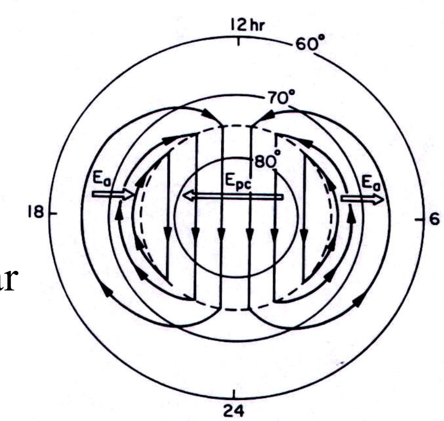

- Motion of day-side reconnected magnetic field gives rise to dawn-dusk E_y field.
  $$\vec{E} = -\vec{V}_{SW} \times \vec{B}_{IMF}$$
- E_y -field maps into the ionosphere $\mathbf{E_{pc}}$ drives anti-sunward flow.
- Reconnection on night-side, leads to field line motion towards the earth in a boundary layer producing electric field $\mathbf{E_a}$ in the dusk-dawn direction.
- Combination of these two electric fields in the ionosphere leads to the Two-Cell convection pattern during southward IMF.

Complex Nonlinear Dynamical Models of Storms and Substorms

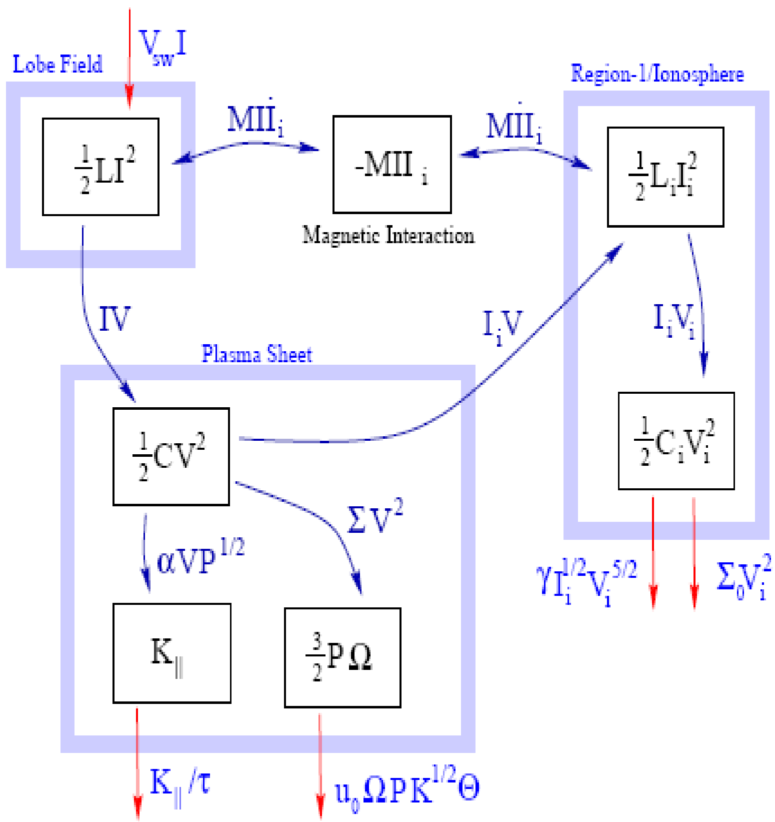

ARMA filters with Kp dependent coefficients 80's, neural nets, SSV

Klimas, Vassiliadis, Baker, 1997

Sharma, Vassiliadis, Papadopoulos

Kamide, Baumjohann, Daglis,Tsurutani +..1998

Solar Wind Driven M-I System

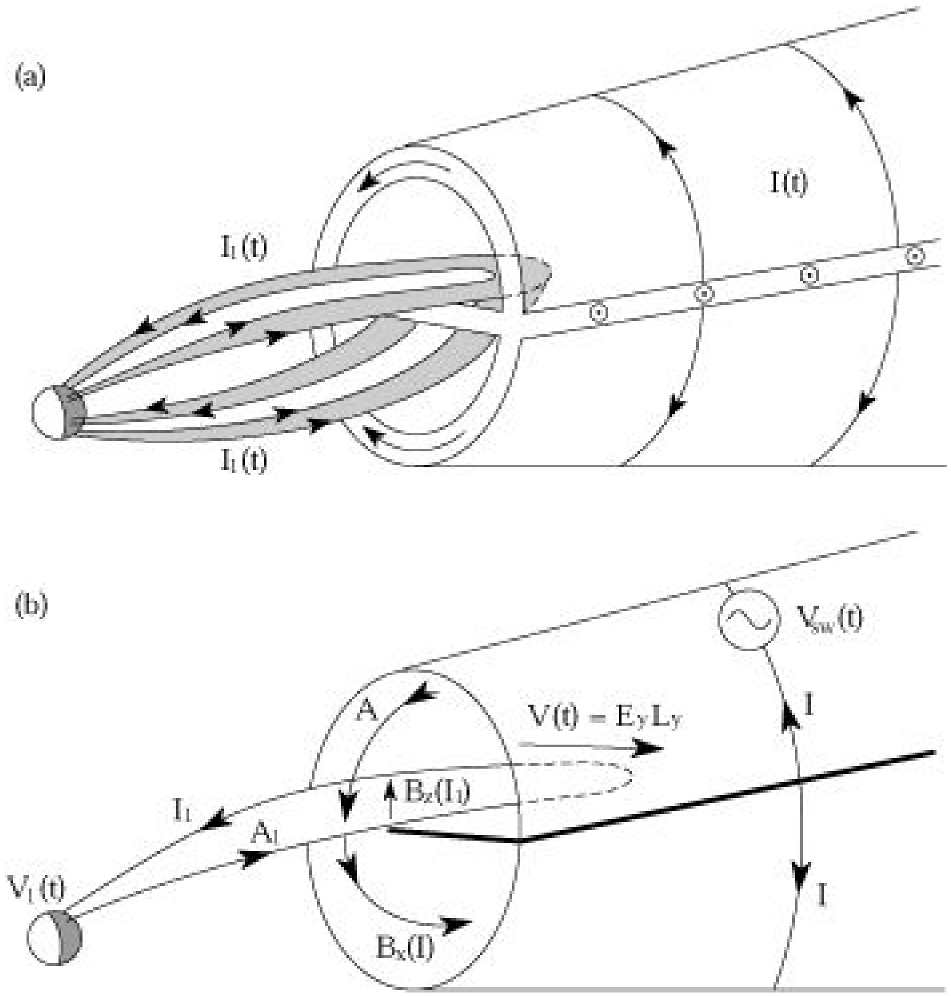

Real-time predictions at
http://ccmc.gsfc.nasa.gov/

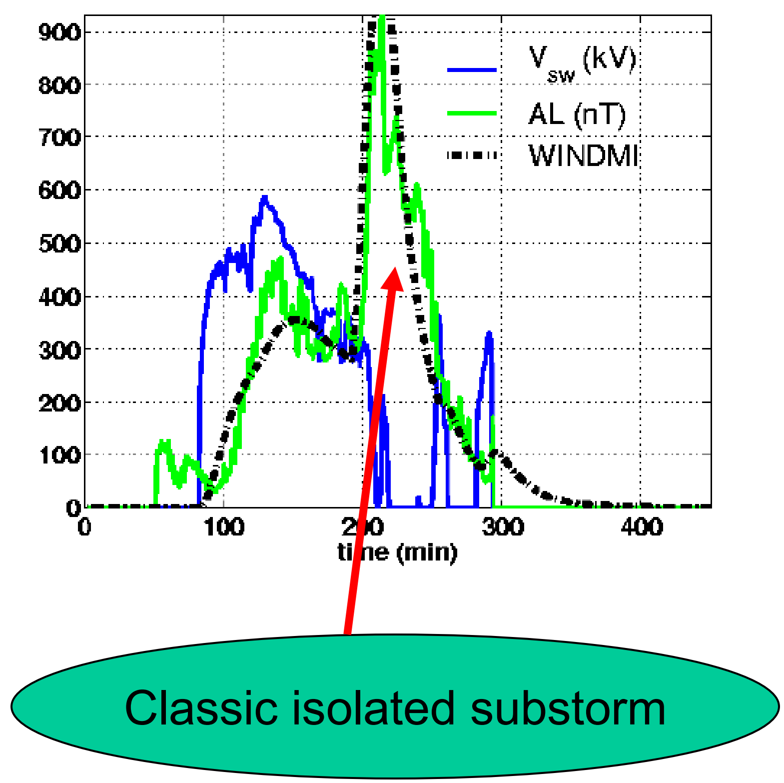

Original models Horton and Doxas, JGR 1996 &1998.
http://orion.ph.utexas.edu/~windmi/realtime/

3D Simulations of Structuring of Polar Cap Patches

$L_z = 1000$ km

$L_x = L_y = 300$ km

V_n=500 m/s neutral wind

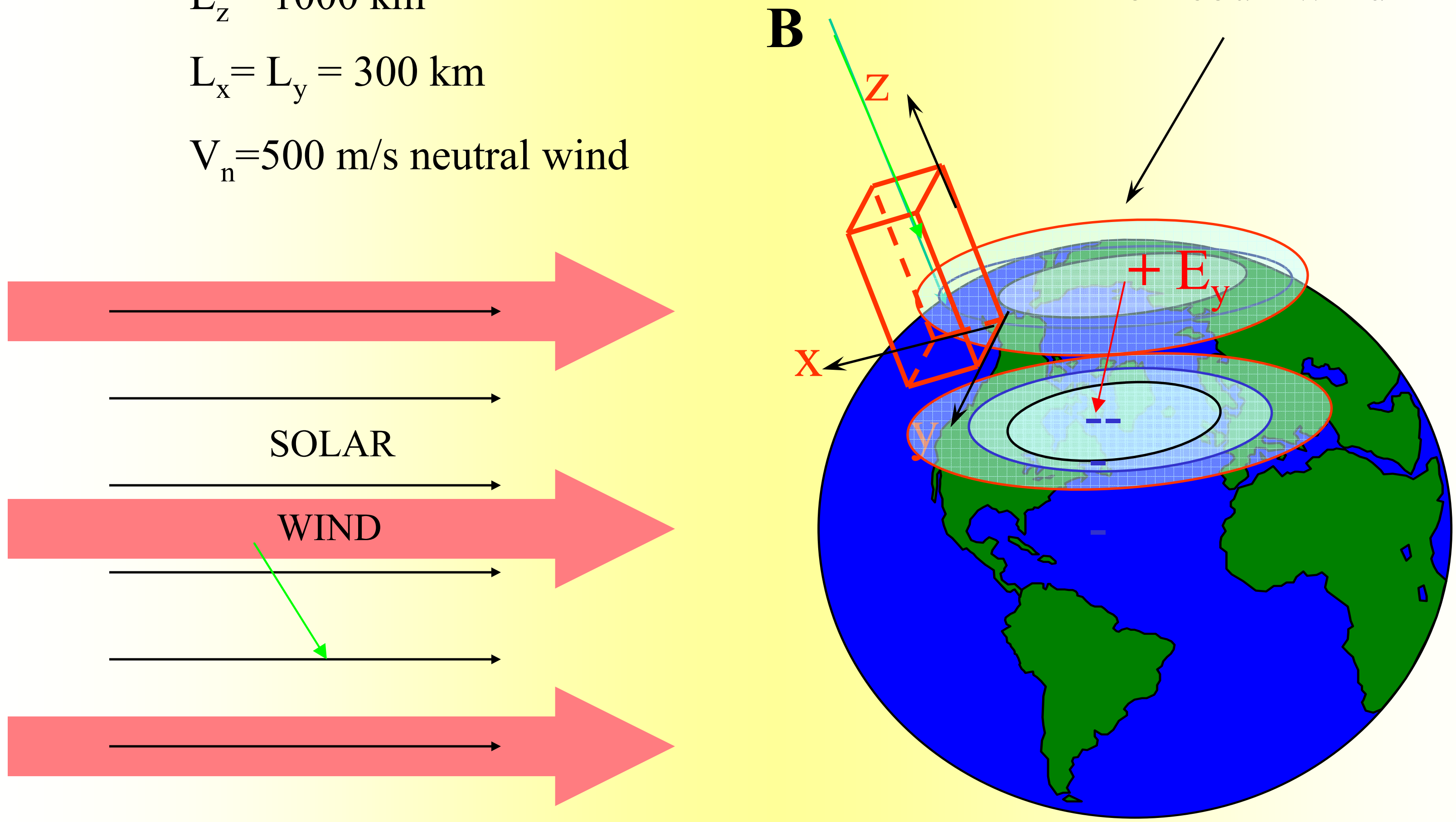

From Parvez Guzdar and Dennis Papadopoulos et al.

Driving Voltages for the AGU Storm of 2006
Comparison of three well known dynamo driving voltages

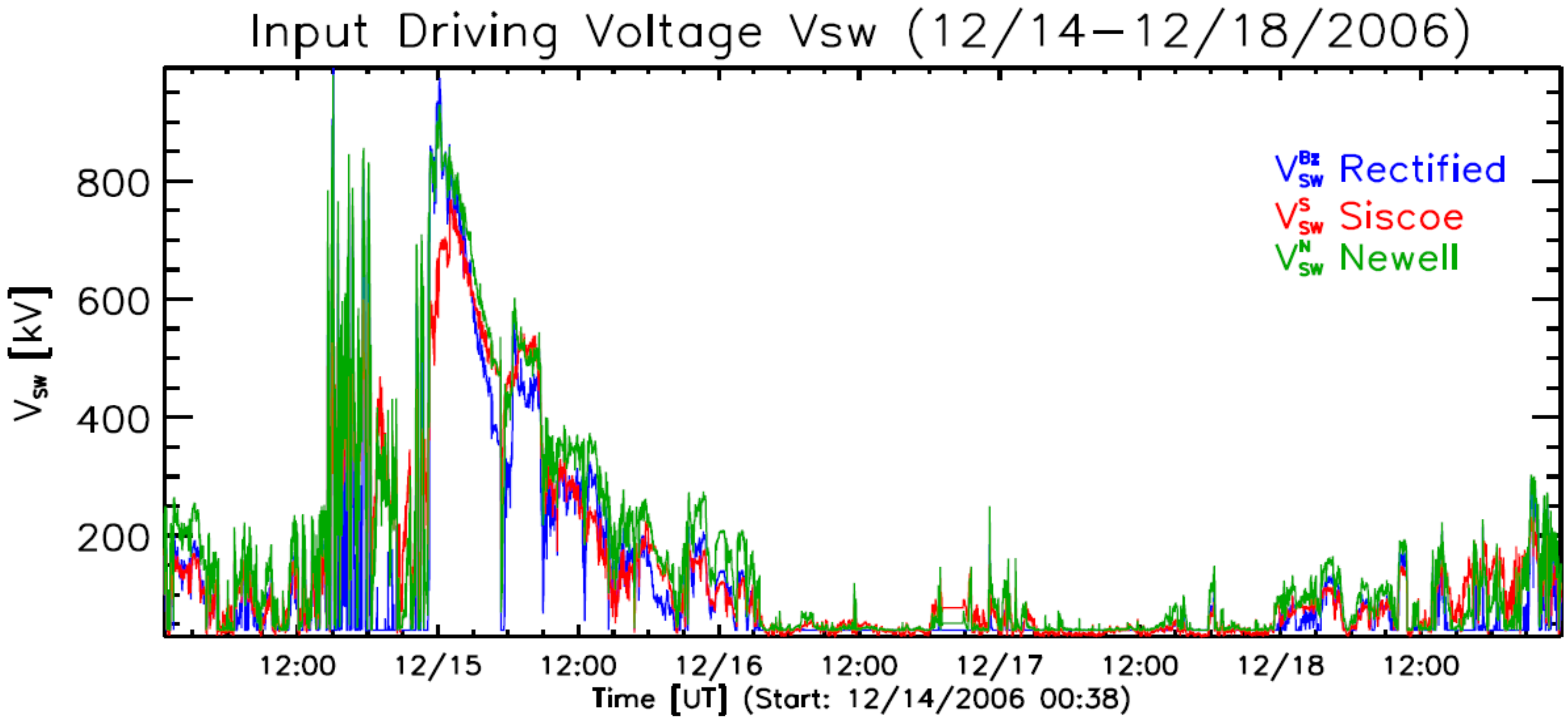

Mays, Horton, Spencer, and Kozyra (2009), *Real-time predictions of geomagnetic storms and substorms: Use of the Solar Wind Magnetosphere-Ionosphere System model, Space Weather*, doi:10.1029/2008SW000459, in press.

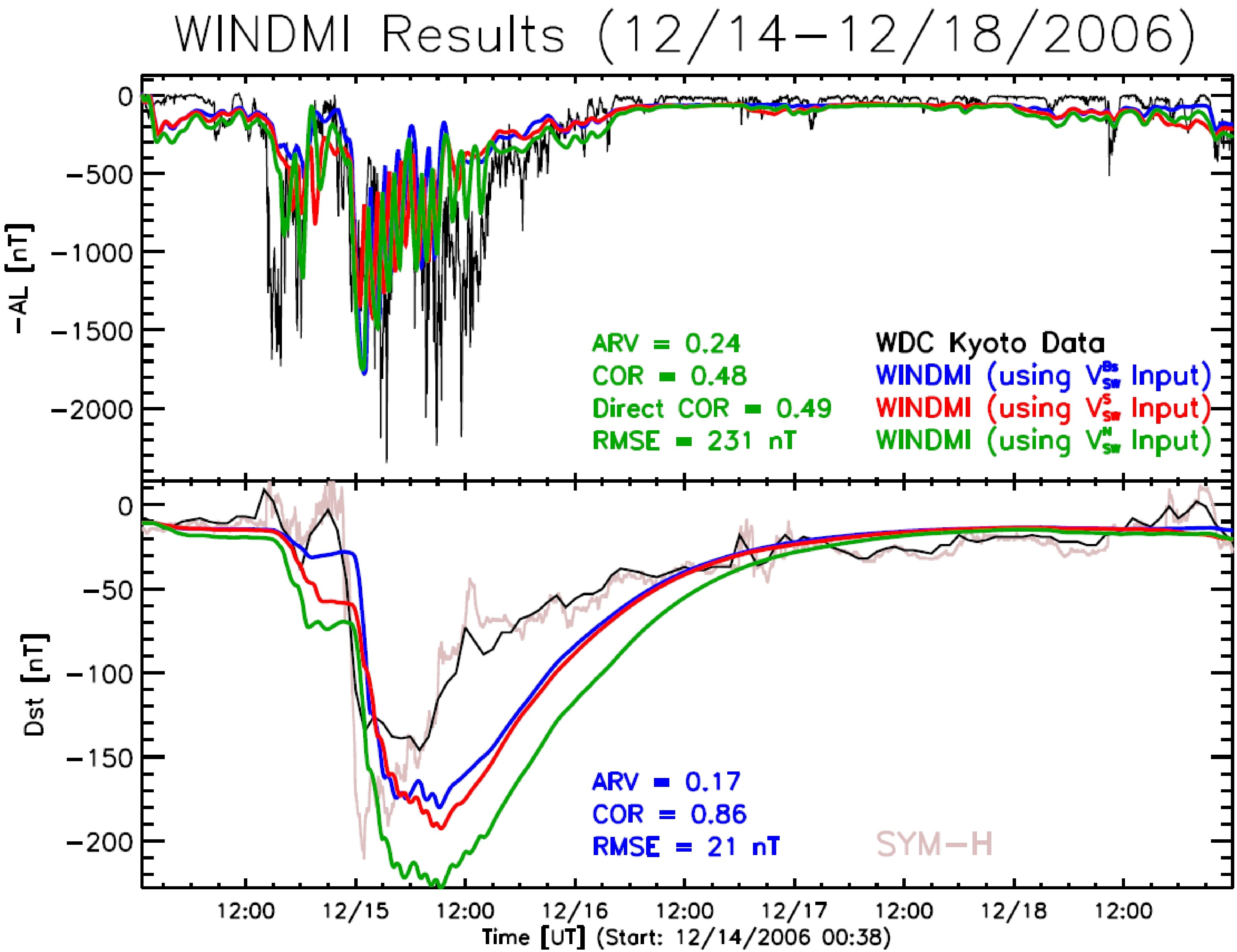
WINDMI Results (12/14–12/18/2006)
−AL [nT]
0
−500
−1000
−1500
−2000
ARV = 0.24
COR = 0.48
Direct COR = 0.49
RMSE = 231 nT
WDC Kyoto Data
WINDMI (using V_{sw}^{Bs} Input)
WINDMI (using V_{sw}^{s} Input)
WINDMI (using V_{sw}^{N} Input)
Dst [nT]
0
−50
−100
−150
−200
ARV = 0.17
COR = 0.86
RMSE = 21 nT
SYM−H
12:00
12/15
12:00
12/16
12:00
12/17
12:00
12/18
12:00
Time [UT] (Start: 12/14/2006 00:38)

Table 3. Mean ARV Measures of Real-Time WINDMI Model Results[a]

Input	Mean *AL* ARV	Mean *Dst* ARV
Rectified V_{sw}^{Bs}	0.38 ± 0.21	0.37 ± 0.27
Siscoe V_{sw}^{S}	0.41 ± 0.16	0.42 ± 0.23
Newell V_{sw}^{N}	0.33 ± 0.17	0.54 ± 0.39

Table 5. Mean Values of the RMSE of Real-Time WINDMI Model Results[a]

Input	Mean *AL* RMSE	Mean *Dst* RMSE
Rectified V_{sw}^{Bs}	123.2 ± 52.4	9.8 ± 3.4
Siscoe V_{sw}^{S}	126.1 ± 45.5	10.7 ± 4.0
Newell V_{sw}^{N}	111.5 ± 39.5	11.9 ± 6.9

Simulations of Pressure Pulses

Pressure wave
introduced deep
(X=-60) in the
tail amplifies
the dp/dx
at inner boundary of
magnetotail ~-15R_E.

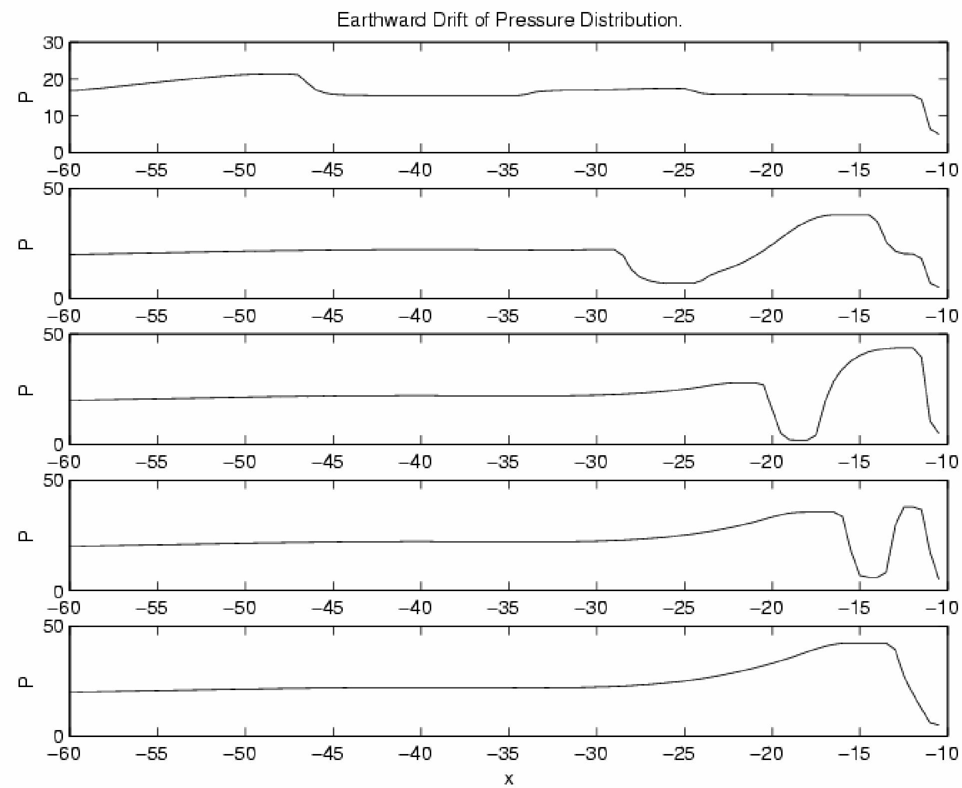

FIG. 4:

Sufficient dp/dx to trigger
interchange/ballooning modes.

$$\frac{\partial}{\partial t}p(x,t) = -\frac{\partial}{\partial \psi}(E_y p - D_\psi \frac{\partial}{\partial \psi}p) - \Gamma p E_y \frac{\partial \ln V}{\partial \psi} + S_{DNL}(t$$

Drift-Ballooning Interchange Modes

1) History of references on two polarizations:

1) **Interchange-Shear Alfven Ballooning** used by Roux, Hurricane-Pellat, Samson, Cheng-Liu, Lee…

Crabtree-Horton-Wong-Van Dam JGR1999, 2007 ..show that most unstable region is at inner edge of plasma sheet…owing to competing stabilizations mechanisms…

2) **Compressional Drift Wave** modes used first by Hasegawa-Chen for mirror modes but extended to gradient modes as Pc5 and Pi2 $\delta B_{\parallel}$ oscillations.

The polarization of the unstable modes is distinguishing feature-of Interchange vs Compressional $\delta B_{\parallel}$ modes.

Drift Mode Characteristics

- Tsyganenko-Stern field models.
- $X=-10$, $L_{pi}=2R_E$, $k_y\rho_i=0.5$, $T_i=5$kev gives

$\omega^*_i \sim 3$mHz $\sim \omega_{D,i}$ below $\omega_{bi} \sim 15$-20mHz

Thus, ion response is time-integral over the bounce-drift orbits with resonance is in ε,μ space.

Typical wavelengths are $2\pi/k_y \sim 20\rho_i \leq 1R_E$.

"Spikes and Bubbles" that accelerate high-δp with the effective-g from field line curvature.

Nonlinear States in Substorms

- Exponential growth till the EXB velocities are comparable to the gc drift velocities. This occurs where MHD-like displacement ξ is of order $2\pi/k_y$ Algebraic growth. [The explosive growth has not been found in ballooning/interchange.]
- Large vortices are formed and fast transport lowers the pressure gradients. Typical fields are $\delta B \sim 5\text{-}10\text{nT}$ and $\delta E_{\perp} \sim 0.1\text{-}1\text{mV/m}$. Sheared background flows control morphology of spikes (blobs) and bubbles.
- Maynard et al AMPTE/CRESS report this type of behavior.

Interchange/Ballooning in Shear Flow

Earth

Y(600km)

$g_{eff} = T_i/m_i R_c$

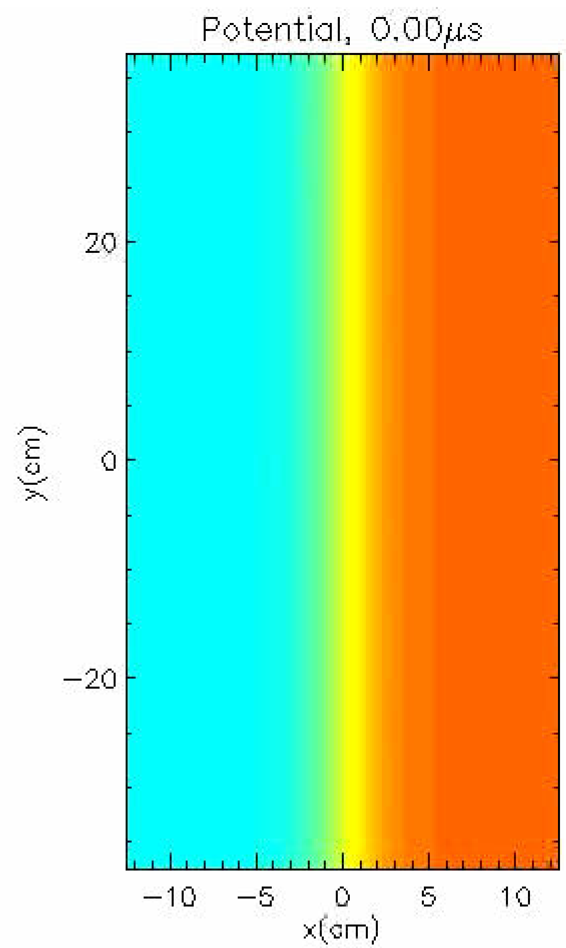

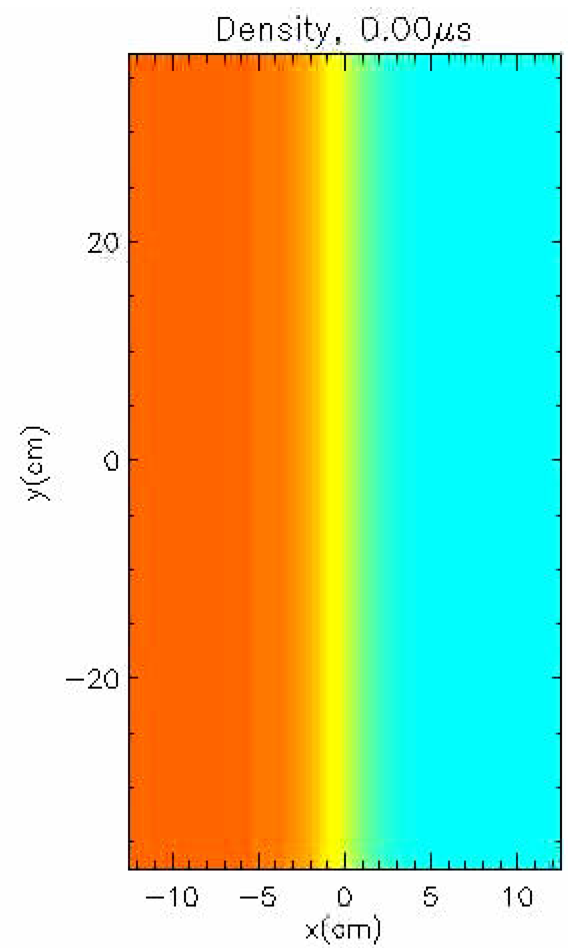

Mid-Tail

Compressional Stabilization

- High beta region beyond ~ 15 R_E is **stable from compression of flux tubes** $\boldsymbol{\delta W \sim \Gamma p (dV/d\psi)^2 \xi^2}$
- Close in to the Earth $X < -6R_E$ plasma is stable.
- The intermediate region $-6 < X < -15\ R_E$ is the first to go unstable as the pressure gradient builds up.
- The 1-D transport model shows the pressure gradient steepening up as the “E&M-fronts” move in to this NGO region. Partly due to v_A increasing.

Nonlinear Bounce-Averaged Analysis

Compressional Drift Modes

- Bounce Averaging of Eq. (4) $|\omega_b| \gg |\frac{\partial}{\partial t}| \sim |\boldsymbol{\delta u}_b \cdot \boldsymbol{\nabla}|$ and taking F_0 to be Maxwellian.

$$\left(\frac{\partial}{\partial t} + i\overline{\omega}_d + \overline{\boldsymbol{\delta u}_b \cdot \nabla}\right)\delta H_k = \left(\frac{\partial}{\partial t} + i\omega_*\right) F_{0M}\overline{\delta\psi_k}$$

Crabtree and Chen 2005.

Crabtree, Horton, Wong, et al JGR, 2002.

- Decomposing $\delta H_k = \delta H_k^l + \delta H_k^{nl}$ where

$$\left(\frac{\partial}{\partial t} + i\overline{\omega}_D\right)\delta H_k^l = \left(\frac{\partial}{\partial t} + i\omega_*\right) F_{0M}\overline{\delta\psi}_k$$

and

$$\left(\frac{\partial}{\partial t} + i\overline{\omega}_D\right)\delta H_k^{nl} = -\overline{\boldsymbol{\delta u}_b \cdot \boldsymbol{\nabla}}(\delta H_k^l + \delta H_k^{nl})$$

- Then Maxwell's equations may be written

$$D_k^l \delta B_{\parallel k} + \sum_j \frac{\beta_j}{2} k_\perp \rho_0 \left\langle v_\perp J_1 \delta H_k^{nl} \right\rangle = 0$$

where D_k^l is the linear eigenmode operator

Sigsbee, Catell, Fairfield, Tsunuda and Kokubun, 2002 JGR

"Geotail Observations of Low Frequency Waves and High Speed Earthward Flows During Substorm Onsets in Near Magnetotail from 10 to 13 R_E"

Lower Hybrid Drift Turbulence, Huba, Gladd and Papadopoulos, JGR **83**, 1978.

Geotail 3s B data for burst ~2000km/s

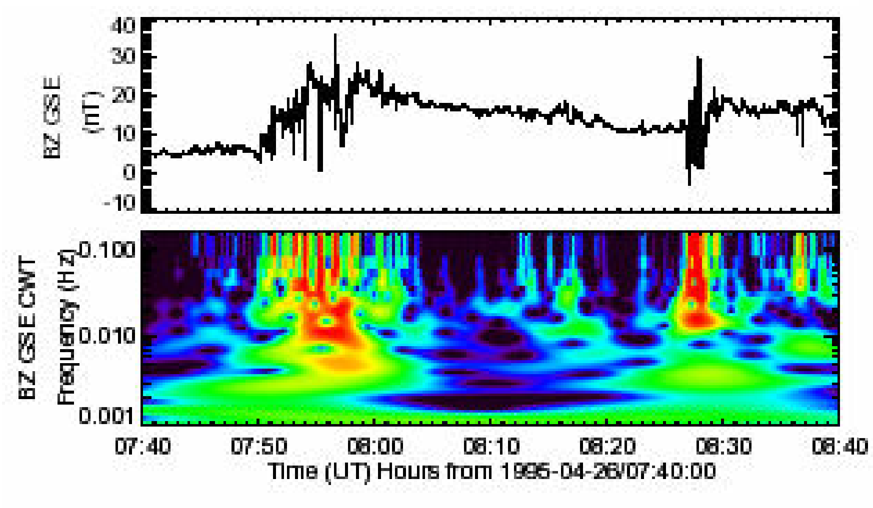

ETS-VI,Dawson,Ft. Simpson Pi2 data

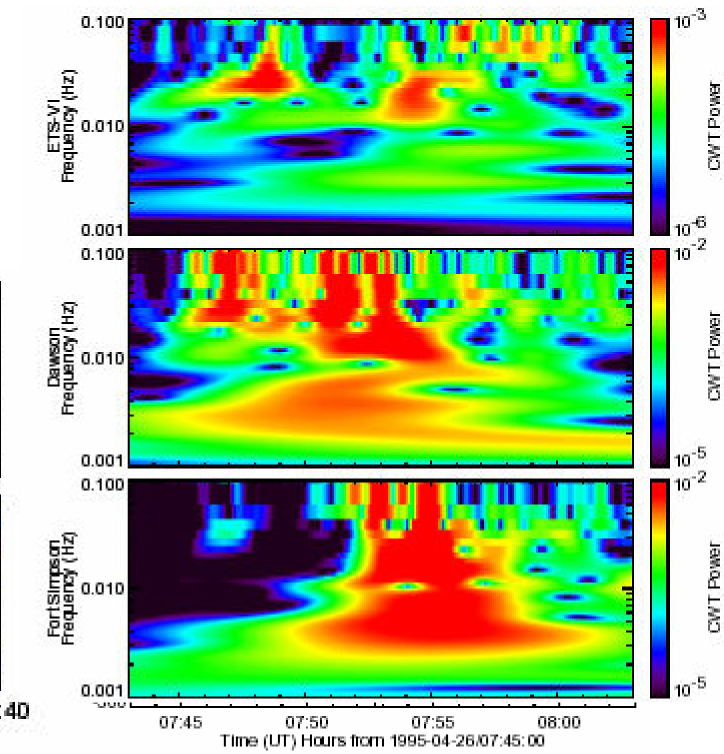

April 26, 1995 Geotail at MLT 23 and x = -13 R_E shows Pi2 oscillations and short bursts of power in ion cyclotron frequency range up to the LHD waves.

Anisotropies: BBF's >Firehose

Fig. 1 of Sigsbee et al JGR 2002

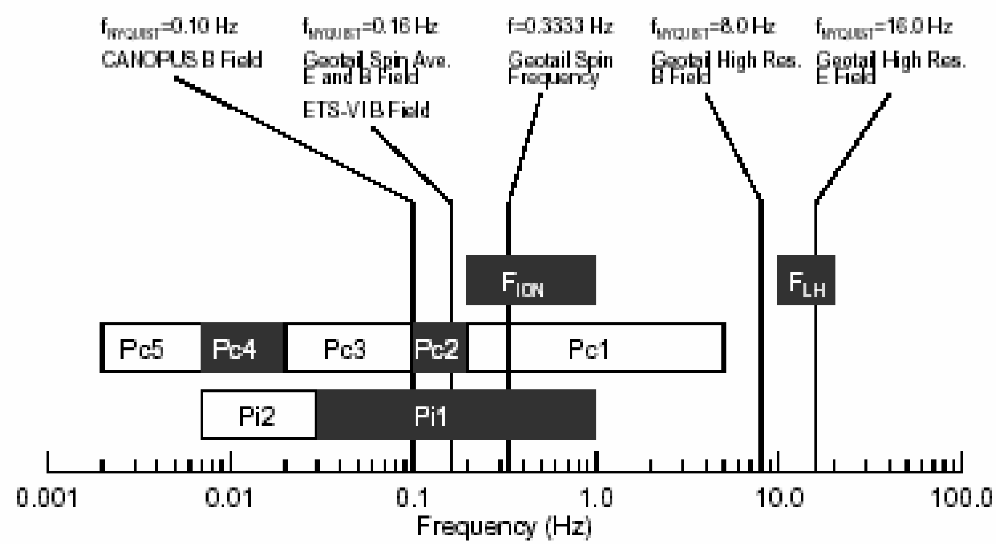

Ji and Wolf (2003) repeated the *Chen-Wolf* (1999) bubble simulation with nonlinear Lagrangian code.

– **A key difference was the development of the firehose instability.**

Nonlinear Firehose Turbulence

$$\delta A_{\pm}(s,t) = \delta A_y \pm i\delta A_x$$

$$\sigma = 1 - \frac{\mu_o (p_{\parallel} - p_{\perp})}{B_o^{\ 2} + \delta B^2}$$

Complex valued fields with large range of behavior from intermittent solitons to wave turbulence. Large amplitude nonlinear δB's in the Pi2 range emitted from the equitorial plane and propagating to the ionospheres.

Hypothesis: FH generates the precursor Pi2 signals from the high speed Earthward flow bursts.

Magnetic Reconnection Models

- Electron Hall MHD- consistient with Cluster 2003 data where separation is 200km.
- Kinetic theory modeling

key space scales $\rho_s = c_s/\omega_{ci}$ and $\delta = c/\omega_{pe}$

vorticity $\varpi = \nabla^2 \varphi(x,z,t)$ current $j = \nabla^2 \psi(x,z,t)$

$$\frac{d}{dt}\rho_s{}^2\nabla^2\varphi = (B_y\partial_y + [\psi,\bullet])\nabla^2\psi$$

$$\frac{d}{dt}(\psi - \delta^2\nabla^2\psi) = -\rho_s{}^2(B_y\partial_y + [\psi,\bullet])\nabla^2\varphi + E_y$$

Four energies:

Mag, EXB, $n_e T_e$,

and $1/2 m_e u_{e\,\parallel}^2$

Hall term 2: electron inertia

Hall term 2: parallel electron pressure gradient

Initial state with small filamentation perturbation $k_z, k_x = (4,1)2\pi/L$

Setup following Bhattacharjee, Wang, Ma, et al.

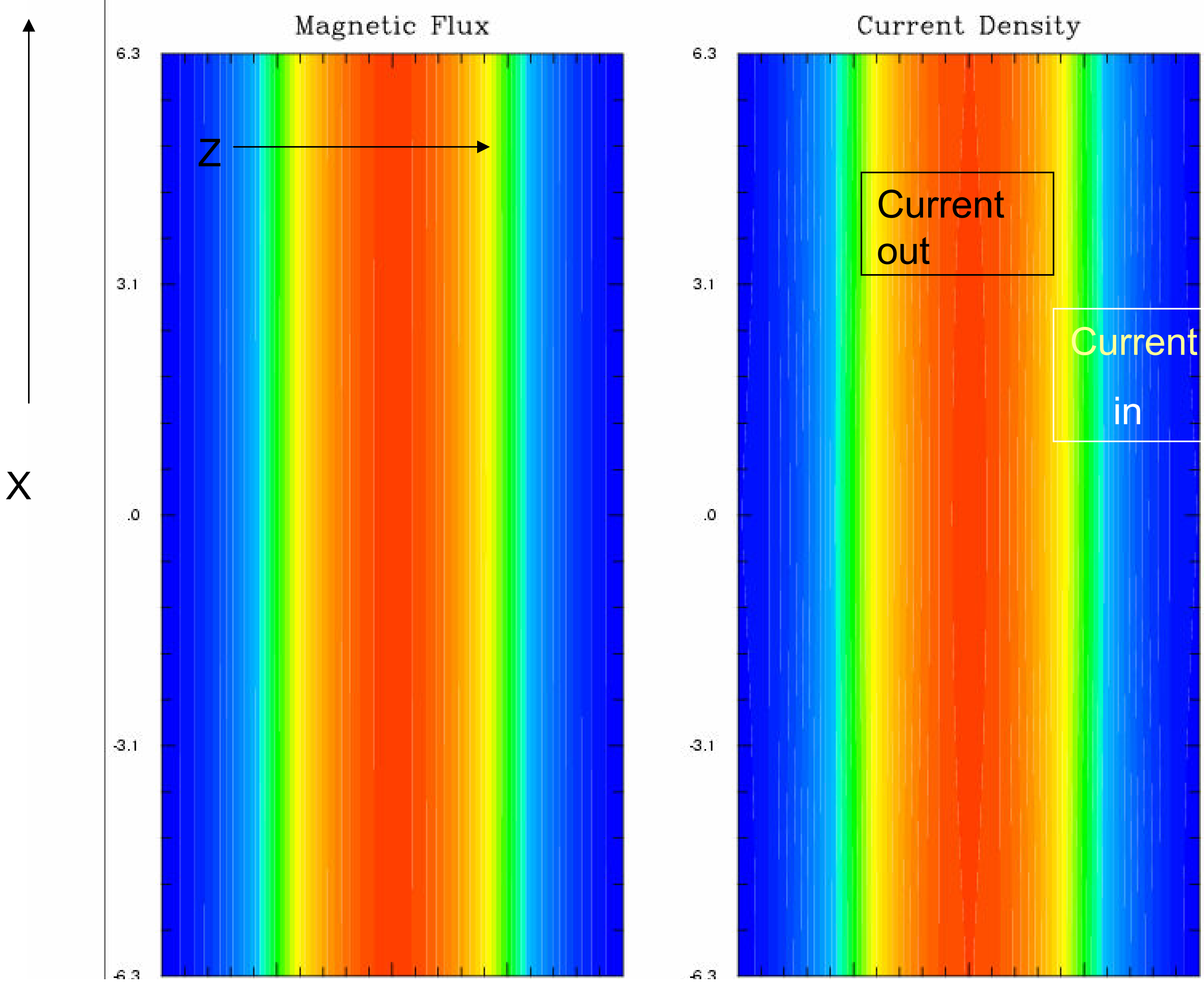

Electron Hall "Dissipationless" Reconnection over time of 110 L_x/v_{alfven} **Explosive Energy Release**

X(10km)

~1200km

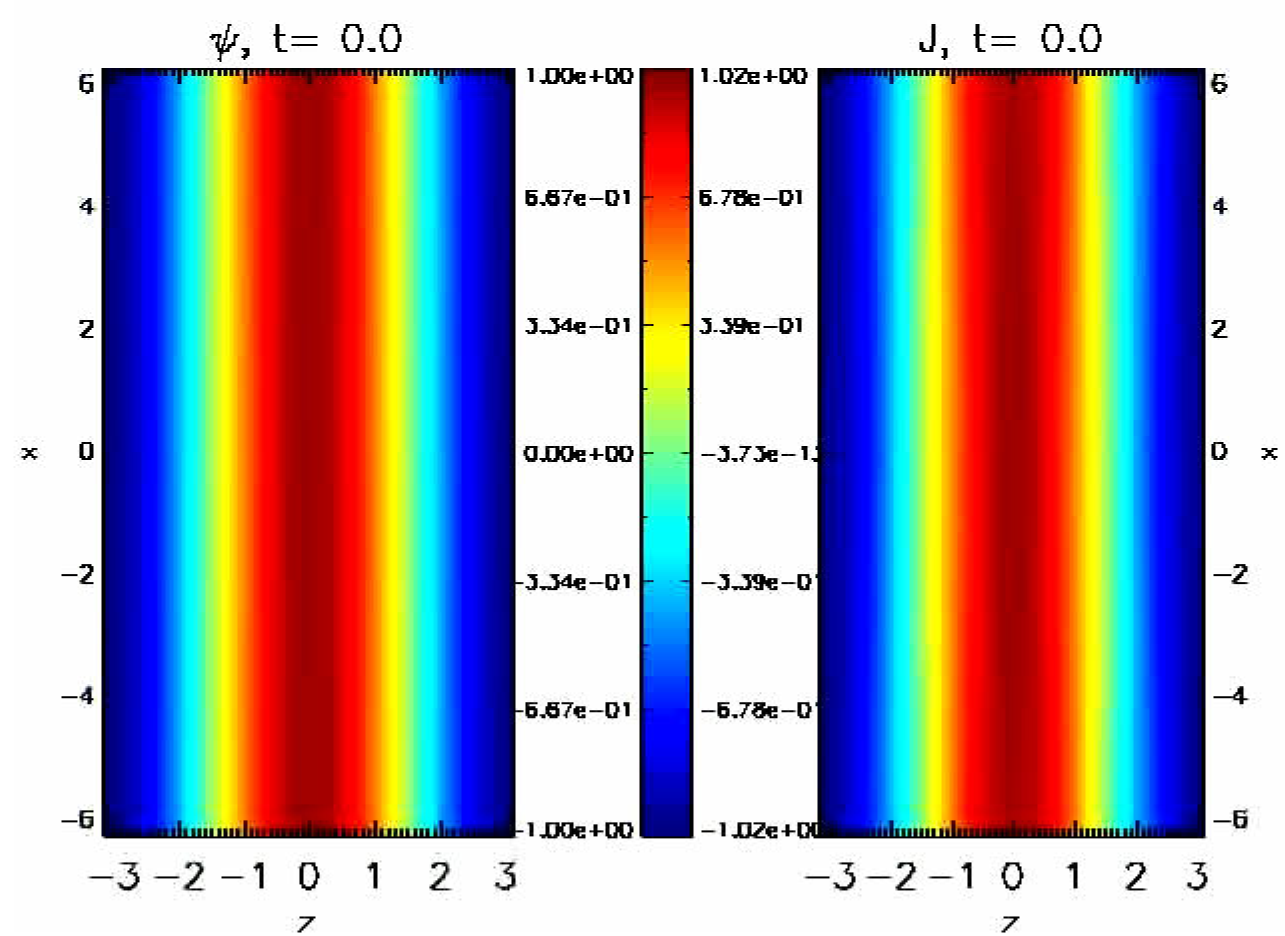

~600km

Z(10km)

Turbulent impulsive magnetic energy release from electron scale

Horton,Kim, Milettello, Ottanviani PHYSICS OF PLASMAS 14, 012902 (2007)

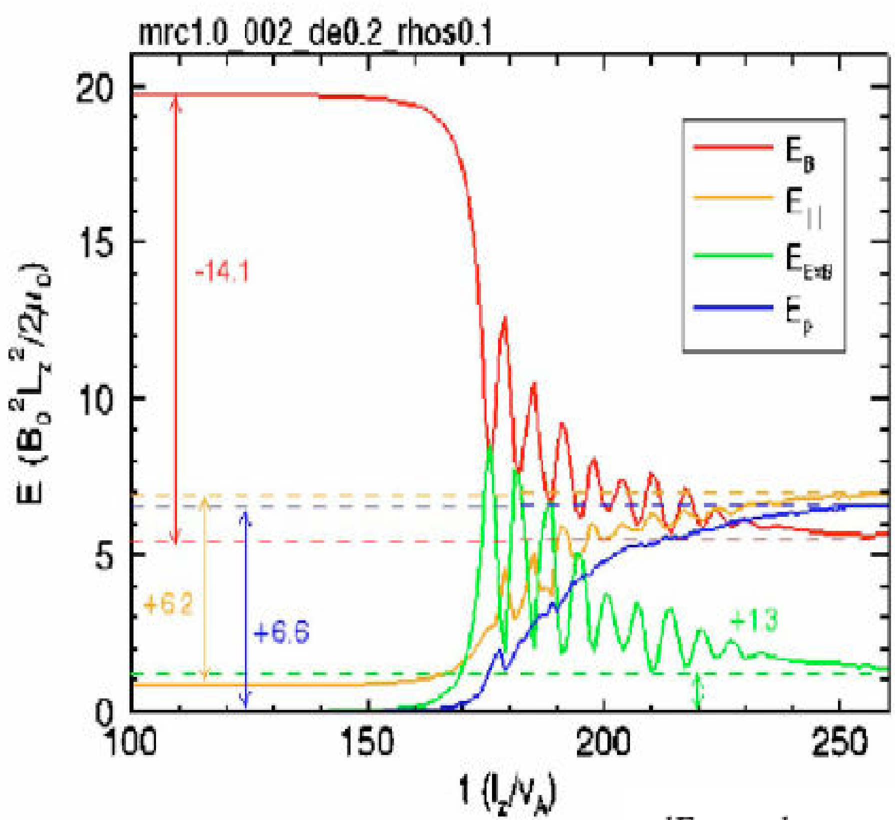

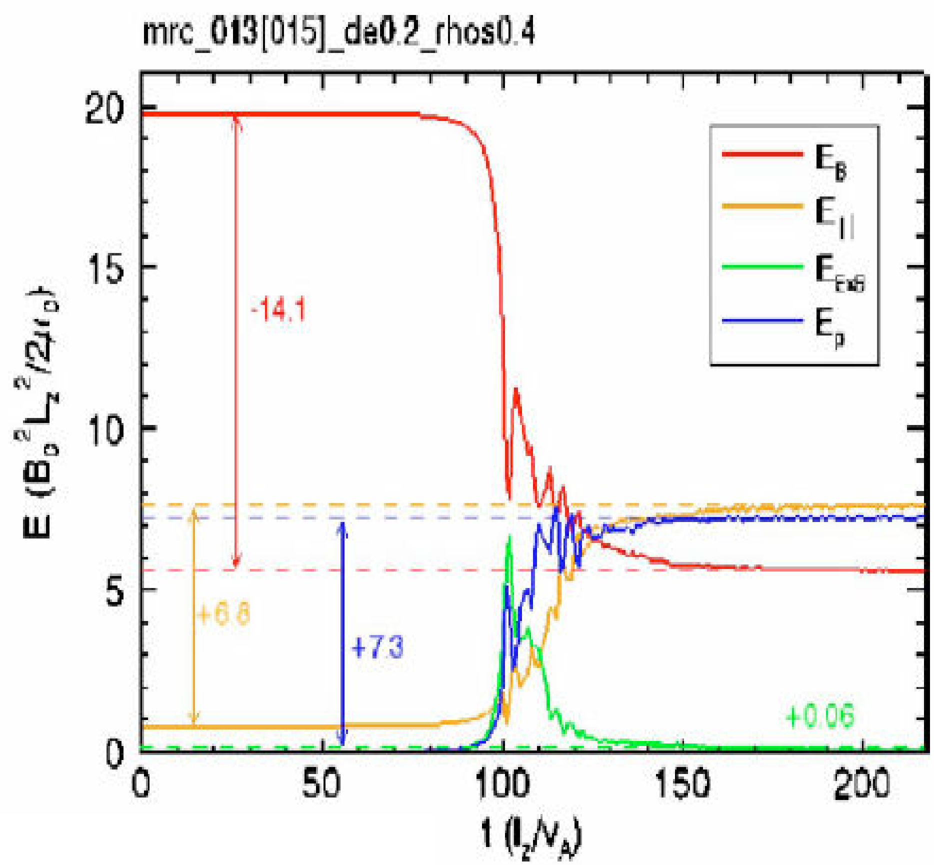

$$\frac{dE_{\text{tot}}}{dt} = \frac{d}{dt}(E_B + E_\parallel + E_{E\times B} + E_p)$$

$$= \frac{1}{2}\frac{d}{dt}\int dxdz\{(\nabla\psi)^2 + d_e^2(\nabla^2\psi)^2 + (\nabla\phi)^2$$

$$+ [\rho_s^2(\nabla^2\phi)]^2\} = 0,$$

Polar Cap Convection Produces Turbulent Ionospheric Density Structures: Guzdar, Gondarenko and Papadopoulos

- Constant Drive (Structuring penetrates through the entire patch)

horizontal structure resolution (x, y) ~ 394 m, 98 m; vertical structure resolution ~ 22 km

Patch: 402 km, 100 km, 1100 km, [1024, 1024, 52];

Gradient
Drift
Instability

Sudan,Gruzinov,,Horton, Kukharkin

Physics Reports 283 (1997) 95–119

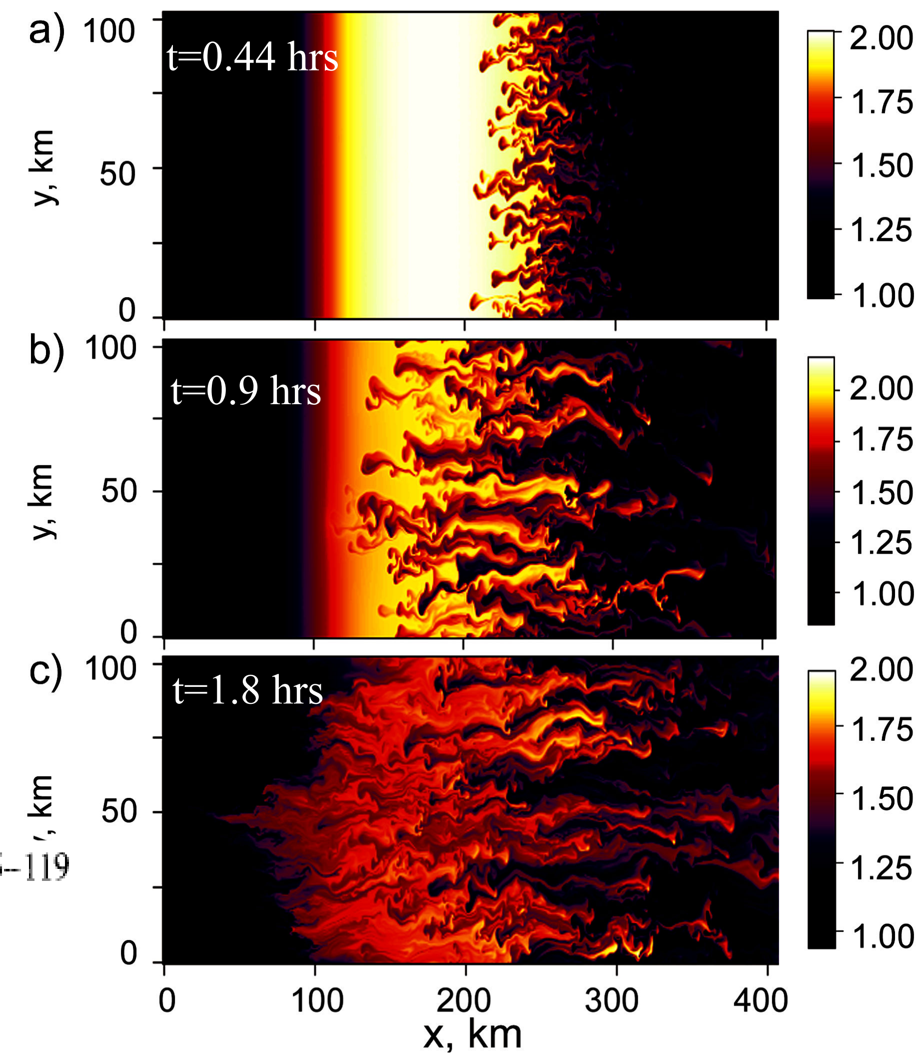

two pde's:

i) vorticity with $v_{neutral}$ wind ~ geff

ii) density

Isomorphic Hasegawa_Wakatani model

Undulations from grad T_i Ballooning Drift Wave

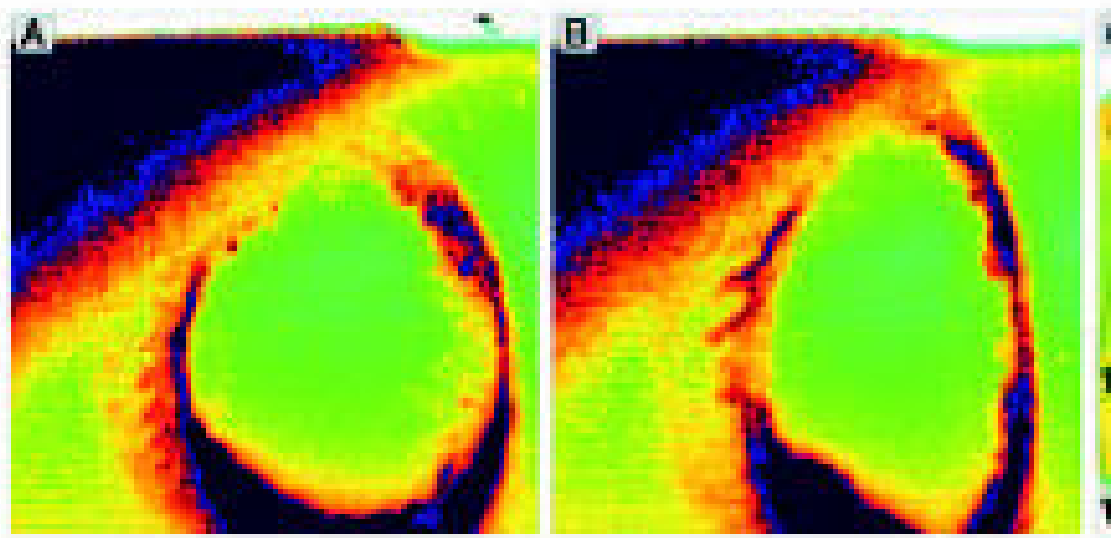

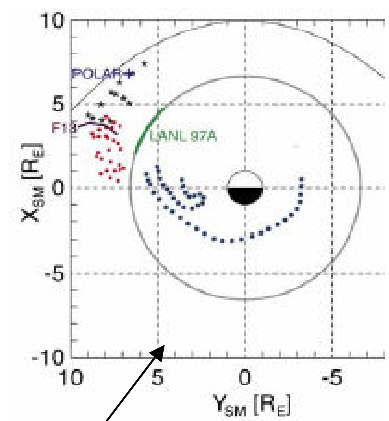

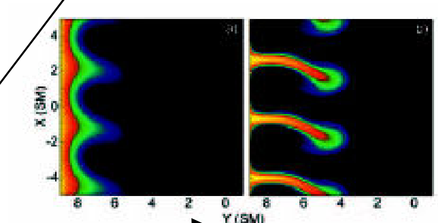

The L=4-9 equitorial plane maps to the images of the fingers in the ionosphere usign Tysganenko and IGRF models.

Lui et al., *JGR* 1987 with AMPTE ion data and by DeMichelis et al., *JGR* 1999 in a statistical study based on the AMPTE ion data.

Theory and Simulations of Auroral Undulations Associated with Instabilities in the Dusk Sector Plasma Sheet

- Undulations were observed on February 6, 2002 along the equatorward edge of the auroral oval with the Far-Ultraviolet Wideband Imaging Camera on NASA's IMAGE satellite during the recovery phase of a moderate magnetic storm.

- The undulations occurred in the 18.5-14.5 MLT sector between 63º and 71º magnetic latitude.

- Their wavelength and crest-to-base length averaged 292 km and 224 km,respectively; and they propagated westward.

- Such undulations are a relatively uncommon auroral phenomenon, and the mechanisms that produce them and the magnetospheric conditions under which they occur are not understood.

W. S. Lewis, J. L. Burch, J. Goldstein, W. Horton, J. C. Perez, H. U. Frey and P. C. Anderson, GRL (2005).

Conclusions

- High order dynamical systems derived and used for real-time forecasting of Space Weather. On the CCMC website as Real-Time forecasts.
- Projection of the PDE's on to key physical variables (pressure, currents and voltages loops) of M-I system leads to networks with conservation laws and bifurcations to substorms and storms.
- "Trigger" switches taken from Kinetic Stability theory. Pass energy between the dynamical cells.
- Multi-Mode Networks are needed to evaluate the role of the competing plasma instabilities in Substorm dynamics and for high resolution Cluster &THEMIS data.

Acknowledgments

- Thanks to Parvez Guzdar and Dimitris Vassiliadis for help preparing the talk.
- NSF supported Space Physics Research at http://orion.ph.utexas.edu/~windmi
- Simulation codes for plasma turbulence at http://pecos.ph.utexas.edu/~vortex

  Similar methods used in tokamaks for bifurcations L, H, ELMy-H, ITB modes.